TRENDS IN SCIENCES 2025; 22(6): 9890 RESEARCH ARTICLE
https://doi.org/10.48048/tis.2025.9890

The Role of Monosodium Glutamate in Neural Crest Cell Migration Impacts Congenital Heart Defects and the Protective Effect of Folic Acid in Chick Embryo Models

Suriyan Pintarasri[1,*], Manutsanun Santiparadon[1], Anussara Kamnate[1], Fatin Ebuh[1], Warisra Nalinbenjapan[1], Firdaws Saising[1,2], Kamonchanok Apitanapipat[1,2] and Nuttakrita Thippheng[1,2]

[1]*Anatomy division, Faculty of Medicine, Princess of Naradhiwas University, Narathiwat 96000, Thailand*
[2]*Medical Education Center Songkhla Hospital, Phawong Subdistrict, Songkhla 90100, Thailand*

([*]Corresponding author's e-mail: suriyan.p@pnu.ac.th)

Received: 29 January 2025, Revised: 6 March 2025, Accepted: 14 March 2025, Published: 5 May 2025

Abstract

Introduction: Congenital heart defects are among the most common birth anomalies, characterized by malformations of cardiac structures such as the pharyngeal arches, aorticopulmonary septum, and outflow tract. Disruptions in neural crest cell function during embryogenesis have been also associated with congenital heart defects. This study investigates the teratogenic effects of monosodium glutamate on the critical signaling pathways of cardiac neural crest cells in cardiac morphogenesis, and folic acid mitigates this adverse effect in chick embryo models. Materials and methods: Using a combined network pharmacology and molecular biology approach, we identified molecular targets potentially associated with monosodium glutamate-induced congenital heart defects. Fertilized chick eggs were divided into control, monosodium glutamate exposure and folic acid treatment groups, and the effects on cardiac tissue structures were evaluated in 3 and 6-day-old embryos. Wingless-related integration site and bone morphogenetic protein signaling proteins were analyzed via immunostaining and immunoblotting techniques, while homocysteine levels were quantified using an ELISA assay. Results and discussion: These findings revealed that the molecular targets shared through network pharmacology and molecular docking analyses were closely linked to neural crest cell function. Monosodium glutamate exposure resulted in a significant reduction in neural crest cell populations and downregulation of Wingless-related integration site and bone morphogenetic protein signaling protein expression ($p < 0.05$). Additionally, homocysteine levels were controlled by monosodium glutamate exposure, suggesting a metabolic influence on cardiac development. Treatment with folic acid mitigates this adverse effect by lowering homocysteine levels. Conclusion: In conclusion, this study provides novel evidence that monosodium glutamate-induced teratogenesis disrupts the protein signaling molecules and metabolic pathways critical to embryonic heart development. This leads to congenital heart defects analogous to those observed in humans. These insights offer a foundation for understanding the impact of environmental teratogens on congenital heart anomalies and the role of neural crest cell-associated signaling pathways in cardiac morphogenesis. Moreover, the treatment with folic acid mitigates an adverse effect on cardiac morphogenesis by lowering homocysteine levels.

Keywords: Congenital heart defects, Monosodium glutamate, Molecular docking, Folic acid, Homocysteine, Cardiac neural crest cell, Chick embryo

Introduction

Arising during embryonic development and present at birth, congenital heart defects (CHDs) are structural anomalies in the heart or great vessels that are leading causes of neonatal morbidity and mortality. Representing the most common congenital malformation globally, CHDs affect approximately 1 %

of live births [1]. Their global birth prevalence is estimated to range between 8 and 12 per 1,000 live births [2]. CHDs are among the multifactorial etiologies involving genetic and environmental factors [3]. Maternal environmental exposures, including dietary components and food additives, are increasingly recognized as potential contributors to CHD risk [4]. Evidence suggests that disturbances in maternal metabolic pathways and oxidative stress induced by exogenous compounds, such as toxins, may disrupt cardiac morphogenesis, and elevated homocysteine levels have garnered attention as a potential teratogen influencing embryonic cardiac development [5,6].

Monosodium glutamate (MSG), widely utilized as a flavor enhancer, has raised increasing concerns about its teratogenic effects, particularly its potential role in CHDs during critical periods of embryonic development [7]. Despite its designation as being generally recognized as safe (GRAS) by the U.S. Food and Drug Administration, concerns have arisen regarding its potential teratogenic effects. Studies suggest that MSG can induce oxidative stress and disrupt the neural crest cells (NCCs) that are critical to embryonic development, including cardiovascular structures. NCCs play a pivotal role in the formation of the heart, and exposure to teratogenic agents like MSG may interfere with their function, leading to CHDs and other developmental anomalies [8,9].

Animal testing has consistently shown that high MSG exposure can lead to developmental toxicity, including structural malformations and altered cardiac development in models such as zebrafish and rodents. For instance, studies on zebrafish embryos demonstrated MSG-induced embryonic defects, highlighting the excitotoxicity and oxidative damage caused by MSG exposure [10]. Similar effects were reported in rat models, in which MSG exposure during gestation led to teratogenic outcomes and heart malformations [11,12]. The teratogenic mechanisms of MSG appear to be linked to its ability to induce oxidative stress and apoptotic pathways, impairing the functioning of critical progenitor cells during organogenesis [13,14]. Moreover, neural crest-derived structures, such as those involved in the cardiac outflow tract, are highly susceptible to teratogenic agents during early developmental windows, making them a key focus of teratological research [15]. Among these, the potential association between MSG exposure during critical periods of embryonic development and CHDs has gained increased scientific attention. This research investigates whether MSG may interfere with key signaling pathways during embryonic heart development.

The advancement of computational biology and systems pharmacology has provided innovative tools that can help to unravel the complex biological interactions underlying multifactorial diseases [16]. Among these, network pharmacology has emerged as a pivotal approach, shifting the paradigm from the traditional "1-drug, 1-target" concept to a holistic understanding of drug actions across multiple targets and pathways [17]. By integrating data from diverse omics platforms, network pharmacology enables the construction of compound-target-pathway networks, offering insights into the molecular mechanisms of bioactive compounds about disease pathogenesis [18]. This methodology is particularly valuable in studying compounds with pleiotropic effects, such as MSG, and their potential implications in conditions like CHDs.

Complementing network pharmacology, molecular docking is a robust computational tool for elucidating structural and functional aspects of compound-protein interactions. By simulating the binding of small molecules to target proteins, molecular docking predicts binding affinities and interaction modes, providing a mechanistic basis for understanding compound activity. In MSG and CHDs, this approach facilitates identifying and validating key molecular targets, such as enzymes, receptors, and transcription factors, which play critical roles in cardiac development [18,19]. Together, these methodologies offer a comprehensive framework for understanding disease mechanisms; applying this framework, we aim to investigate the biological effects of MSG and its metabolites, enabling researchers to explore the intricate molecular networks and interactions that contribute to CHDs.

Cardiac neural crest cells (cNCC) are a specialized subpopulation of neural crest cells that play a crucial role in the development of the heart and great vessels [20]. Originating from the dorsal neural tube at the level of the hindbrain, encompassing the third through sixth pharyngeal arches during embryogenesis, cNCCs migrate extensively to contribute to the formation of

cardiac structures, including the pharyngeal arches, aorticopulmonary septum, and outflow tract (OFT) [21]. Following epithelial-to-mesenchymal transition (EMT), cNCCs migrate ventrally and interact with other cell populations to orchestrate the formation of cardiac structures [22]. This migration is tightly regulated by signaling pathways such as Wnt, BMP, and FGF, which ensure the proper guidance and integration of cNCCs into their target tissues [23].

The multifaceted functions of cNCCs in cardiac morphogenesis have been the focus of extensive research due to the dysregulation of cNCC signaling pathways during embryonic development being strongly associated with CHDs, the most common congenital anomalies globally. We, therefore, aim to explore the role of cNCCs in cardiac morphogenesis, the signaling pathways that regulate their function, and determine which perturbations contribute to CHDs.

The present study aimed to investigate whether MSG and its metabolites disrupt key signaling pathways during embryonic heart development and the treatment role of folic acid in a chick embryo model that most closely resembles human development. Moreover, to understand the heterogeneity of CHDs and explore common molecular targets and signaling pathways, we sought to identify the molecular targets and pathways influenced by MSG, focusing on their contribution to CHDs.

Materials and methods

Chemicals and antibodies

MSG was purchased from Sigma-Aldrich (USA). The 4 mg of MSG solution was prepared as described in a previous protocol [24]. Anti-HNK-1 antibody (SIG-C6680, mouse monoclonal), anti-BMP-2 antibody (SIA-ZRB1489, rabbit monoclonal), anti-Wnt10B antibody (SIA-SAB5300003, mouse monoclonal), and secondary antibody conjugated-HRP (AP124P, goat anti-mouse) were purchased from Merck Millipore. Fluorescein-conjugated secondary antibodies Goat Anti-Rabbit IgG (Alexa Fluor® 488, ab150077) and Goat Anti-Mouse IgG (Alexa Fluor® 594, ab150116) were purchased from Abcam (UK). The Human Homocysteine Elisa kit (Cat no. MBS7252797) was purchased from BioSource (USA).

Chick embryo experiments

This research received approval from the Walailak University Institutional Animal Care and Use Committee (WU-IACUC), number WU-ACUC-65029. The 300 freshly laid fertilized eggs (*Gallus gallus domesticus*) were cleaned with sterile water and weighed. Then, all fertilized eggs were divided into the control group (0.9 % NSS, n = 20; and 0.6 mg/kg FA, n = 20), the experimental group (4 mg of MSG, n = 20) and treatment group (4 mg of MSG plus 0.6 mg/kg FA, n = 20). The eggs were then incubated at 39 ± 0.5 °C with 50 - 60 % humidity in a humidified incubator and turned 120 ° automatically thrice daily. A single injection of 50 µL soluble agent was delivered into the fertilized eggs after 21 h of incubation using the ovo-injection method. In addition, embryonic death, unfertilized eggs, cracked shells, and eggs weighing less than 60 g. were excluded.

Identification of potential targets for MSG and CHDs

The SMILES (simplified molecular-input line-entry system) codes of MSG were obtained from PubChem (https://pubchem.ncbi.nlm.nih.gov/) and the STITCH database (http://stitch.embl.de/). A total of 129 targets were obtained after removing duplicates and these were then imported to the Swiss Target Prediction database (http://www.swisstargetprediction.ch/) to predict the molecular targets. The target information related to CHDs was identified from the GeneCards (https://www.genecards.org/) and OMIM (http://bionet.ncpsb.org.cn/batman-tcm/) databases. After deleting the duplicate targets, a total of 14,910 targets closely related to the occurrence and development of CHDs were stored. A Venn diagram drawing was used to identify targets between MSG and CHDs overlapping (https://bioinformatics.psb.ugent.be/webtools/Venn).

Network construction

Protein-protein interaction (PPI) between MSG and CHD-targeted proteins was analyzed using the STRING database (https://string-db.org/cgi/input.pl) (PPI combined score > 0.4). Cytoscape software (https://cytoscape.org/) was used for the PPI network visualization and critical protein identification. The importance of targets was determined by degree.

KEGG pathway enrichment

KEGG (Kyoto Encyclopedia of Genes and Genomes) enrichment pathway analysis was performed in ShinyGO 0.81 free online software (http://bioinformatics.sdstate.edu/go77), and enrichment visualization was displayed using Cytoscape software. For the KEGG analysis, $p < 0.05$ was considered a significant enrichment. The enrichment results of KEGG analyses were generated in a bubble chart and bar graph.

Molecular docking analysis

AutoDock tools were used to perform a molecular docking study of the MSG and targeted proteins. The mol2 file MSG was downloaded from PubChem, and the structures of targeted proteins were downloaded from the RSCB Protein Data Bank (PDB) database. Molecular docking was performed in AutoDock Vina according to the manufacturer's manuals. PyMol software was used to analyze and visualize the docking results. Protein domains were predicted by analyzing amino acid sequences using LigPlot+ v.2.2-ligand-protein interaction diagrams (https://www.ebi.ac.uk/thornton-srv/software/LigPlus/).

The histological study

The whole body of living ED-3 and ED-6 were fixed with 4 % paraformaldehyde in PBS, processed, and embedded in paraffin wax. The paraffin block was sectioned at 6 µM. The tissue sections of each group were stained with hematoxylin and eosin (H&E), observed under a light microscope (Olympus BX53, Japan), and photographed.

Immunohistochemistry staining

To investigate the NCCs on 3-day-old embryos (ED-3), sections of ED-3 paraffin-embedded tissue were dewaxed, rehydrated, and retrieved using 10-mM sodium citrate buffer (pH 6.0) for 20 min. Sections were then rinsed in PBS, and a protein blocker (Vector, USA) was applied for 5 min to block nonspecific background staining. Sections were incubated at 4 °C overnight with the anti-HNK-1 (1:100), a specific marker of NCCs. The slides were washed with PBS and incubated with the secondary HRP-conjugated antibody (1:500) for 4 h. The slides were then washed in PBS, incubated with DAB Substrate (Vector, USA) for 20 min at room temperature, and then counterstained in Mayer's hematoxylin for 30 s. The slides were observed under a light microscope (Olympus BX53, Japan) and photographed.

Immunofluorescence staining

The protein Wnt and BMP signaling of the NCCs was determined using the colocalization of anti-HNK-1, anti-Wnt10B, and anti-BMP-2 protein signaling on ED-3 embryos. Briefly, sections of paraffin-embedded tissue were dewaxed, rehydrated, and retrieved using 10-mM sodium citrate buffer (pH 6.0) for 20 min. Subsequently, the tissues were permeabilized with 0.1 % Triton X-100 for 10 min at room temperature, washed 3 times with PBS, blocked with PBS containing 5 % bovine serum albumin for 1 h, and incubated overnight at 4 °C in a humidified chamber with primary antibodies against HNK-1 (1:100), Wnt10B (1:100), and BMP-2 (1:100). Next, the slides were washed with PBS and incubated with the fluorescein-conjugated secondary antibodies (1:500) for 30 min. DAPI was used for counterstaining. The slides were washed with PBS and mounted using 50 % glycerin in PBS. The slides were visualized by a fluorescence microscope equipped with a camera (Olympus), photographed, and measured for their mean fluorescence intensity using the Fiji program.

Elisa-homocysteine determinations

BDs result from unrelated amounts of homocysteine (Hcy), folate, and vitamin B12, resulting in higher amounts of Hcy and abnormalities in the embryo. Studies conducted on animal subjects have shown that a decrease in folate is associated with an increase in Hcy in the bloodstream, resulting in abnormalities in the embryo [25]. We further estimated the quantitative Hcy levels in tissues extracted from the cardiac region of chick embryos. The tissue-Hcy from the experiment (MSG), the treatment (MSG + FA) and the control groups (NSS and FA) of embryos were extracted and examined with the Human Homocysteine Elisa kit (Cat no. MBS7252797, BioSource, USA). Five ED-6 embryos from each group were dissected and collected under a stereo microscope (Olympus model SZ61, Japan). Next, tissues were rinsed thoroughly in ice-cold PBS with a pH 7.2 to remove excess blood before homogenization. The tissues were then minced into small pieces and homogenized on ice in 200 µL of

cold PBS with glass tissue grinders (PYREX® Potter-Elvehjem tissue grinders). The resulting suspension was ultrasonicated for 10 min to break the cellular membrane further. After that, the homogenates were centrifuged twice at 5,000 rpm for 15 min each time at a temperature of 4 °C (Eppendorf model 5424R, Canada). The supernatant and assay were collected immediately with the Human Homocysteine Elisa kit. The tissue-Hcy supernatant was measured for optical density (O.D.) at 450 nm by a photometer microplate (CLARIOstar® Plus model, BMG Labtech, Germany), and the results were their mean analyzed for statistical analysis using the Prism version 9 program.

Statistical analysis

The sample size was calculated by Statsols, a provider of n-Query Advisor, based on the number of mortality rate estimations in ED-3, which was 20 in each group. All experiments were performed in triplicate, and the data was analyzed using version 9 of Prism software. All data were expressed as mean ± SD. Differences in the measured parameters in the different studied groups were tested using the 1-Way ANOVA followed by the post-hoc Tukey HSD (Honestly Significant Difference) test, and significance was considered at $p < 0.05$.

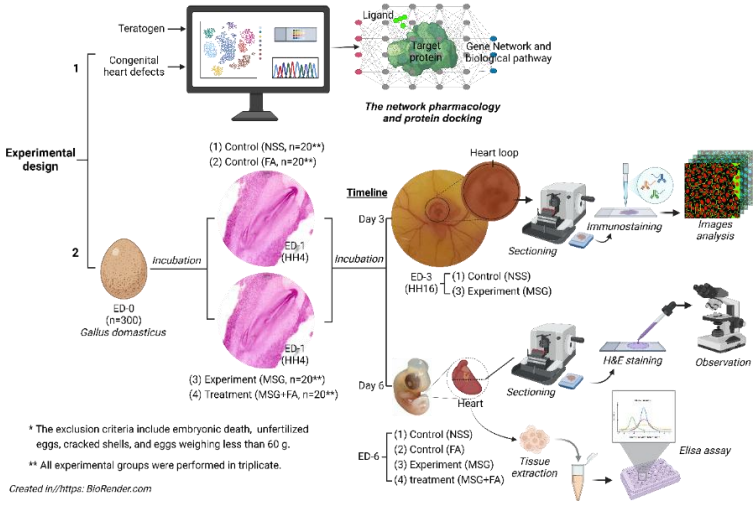

Figure 1 Experimental design for evaluating MSG role induced congenital heart defects by computational and experimental analysis.

Results and discussion

Identified the network pharmacology approach of teratogenic compounds and their potent target-induced CHDs

Prediction of selected overlapping between MSG and CHD targets

This study focused on the food additive MSG, which induces CHDs. The corresponding potential targets related to MSG exposure (28) and CHDs (14,910). As shown in **Figure 2(A)**, there were 2 overlapping MSG and CHD targets in the Venn diagram. A total of 20 shared genes were identified, underscoring their potential role in mediating pathways linking MSG exposure to CHD pathogenesis.

Protein-protein interaction, KEGG enrichment analysis, and PPI network

Functional enrichment analysis revealed a strong association with various signaling pathways, including glutamate receptor activity, GPCR activity, and transmembrane signaling receptor activity. This suggests that these processes are critical mediators of disease development. These pathways involve molecular transducer activities that may disrupt cellular communication and development during cardiogenesis.

Furthermore, the gene network analysis emphasized the involvement of glutamate receptor signaling and neurotransmitter pathways, which are potentially linked to neurodevelopmental disorders, cardiomyopathies, and specific structural heart defects, such as atrioventricular defects, atrial septal defects, and

tetralogy of Fallot, as shown **Figures 2(B) - 2(E)**. These findings align with the hypothesis that disruption of signaling processes, particularly those regulated by glutamate receptors and GPCRs, could contribute to abnormal cardiac development and associated neurodevelopmental phenotypes.

In conclusion, this study provides novel insights into the mechanistic connections between MSG exposure and CHDs through shared molecular pathways and functional networks. These results highlight the need for further experimental validation and exploration of the role of the identified signaling pathways in CHD pathogenesis. This may then open avenues for targeted interventions and improved understanding of environmental contributions to congenital disorders.

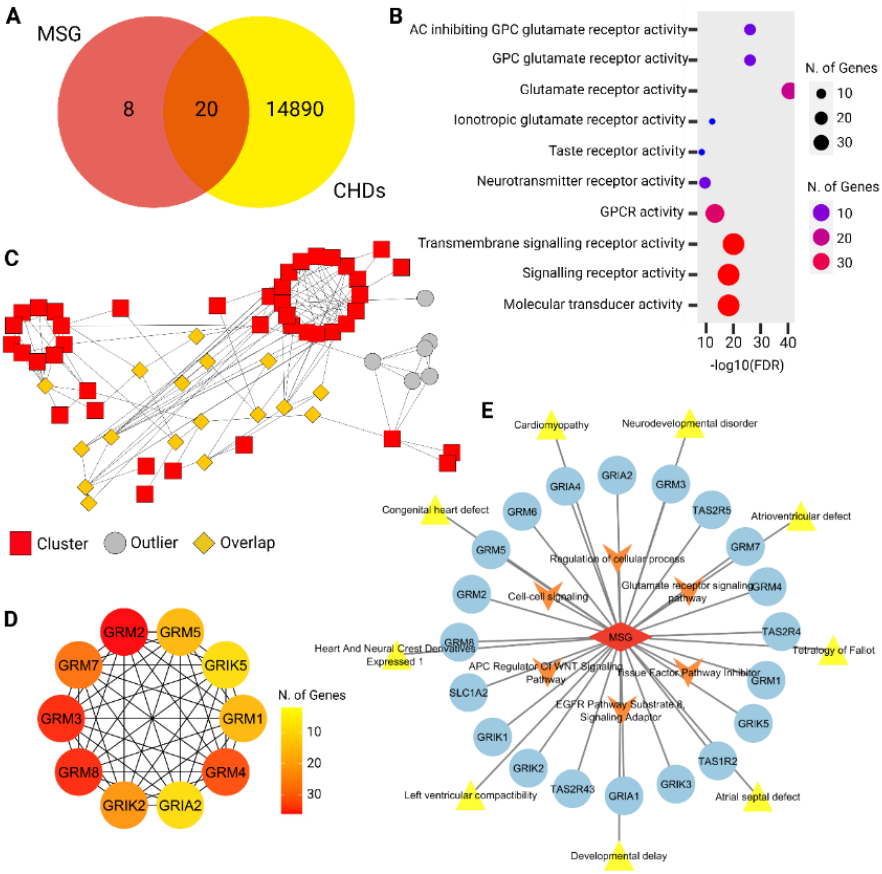

Figure 2 The network pharmacology-based approach of the targets of MSG and CHDs. (A) Venn diagram of 28 targets of MSG and 14,910 targets of CHDs. Two common targets between the targets of MSG and CHDs were identified as candidate targets of MSG in the induction of CHDs. Go and KEGG enrichment analyses were performed on the 129 predicted targets of MSG in the induction of CHDs. The bar graph (B) corresponds to the predicted targets in biological processes, cellular components, and molecular function. The enrichment bubble plot of gene numbers corresponds to the bar graph (the more significant the nodes, the darker the color, and the more the genes were enriched). PPI network of MSG - signaling pathway-target protein - CHDs networks. (C) A molecular or gene interaction network is visualized, where the red squares represent key nodes (likely genes or proteins), and the yellow diamonds may represent intermediary functional annotations or pathways. Highly interconnected nodes (hubs) suggest their central role in the network. (D) The top 10 proteins with the highest node degrees were analyzed from 129 nodes and 14,910 edges. The color gradient reflects varying levels of significance or fold change, with red indicating a stronger association. (E) The blue nodes show the 20 proteins, with the light green nodes representing the hub genes, and the orange nodes being the pathways associated with the core target nodes and 14,910 edges. The color gradient reflects varying significance levels or fold-change, with red indicating a stronger association. (E) The blue nodes show the target proteins, while the light green nodes represent the hub genes, and the orange nodes are the pathways associated with the core targets.

Molecular docking

Molecular docking was used to evaluate the binding affinity between MSG and 10 different related targets, namely glutamate metabotropic receptor subunit 1 - 5, 7 and 8 (GRIM), glutamate ionotropic receptor kainate type subunit 2 and 5 (GRIK), glutamate ionotropic receptor AMPA type subunit 2 (GRIA), and protein coding gene (SLC1A1 and TAS1R3). Regarding the binding energy values, the lower the binding energy value, the higher the interaction stability; MSG had the strongest binding affinity with the 3 different-related targets, as shown in **Figure 3**. Furthermore, the corresponding amino acids involved in the interactions between MSG and 10 related targets are demonstrated in **Table 1**.

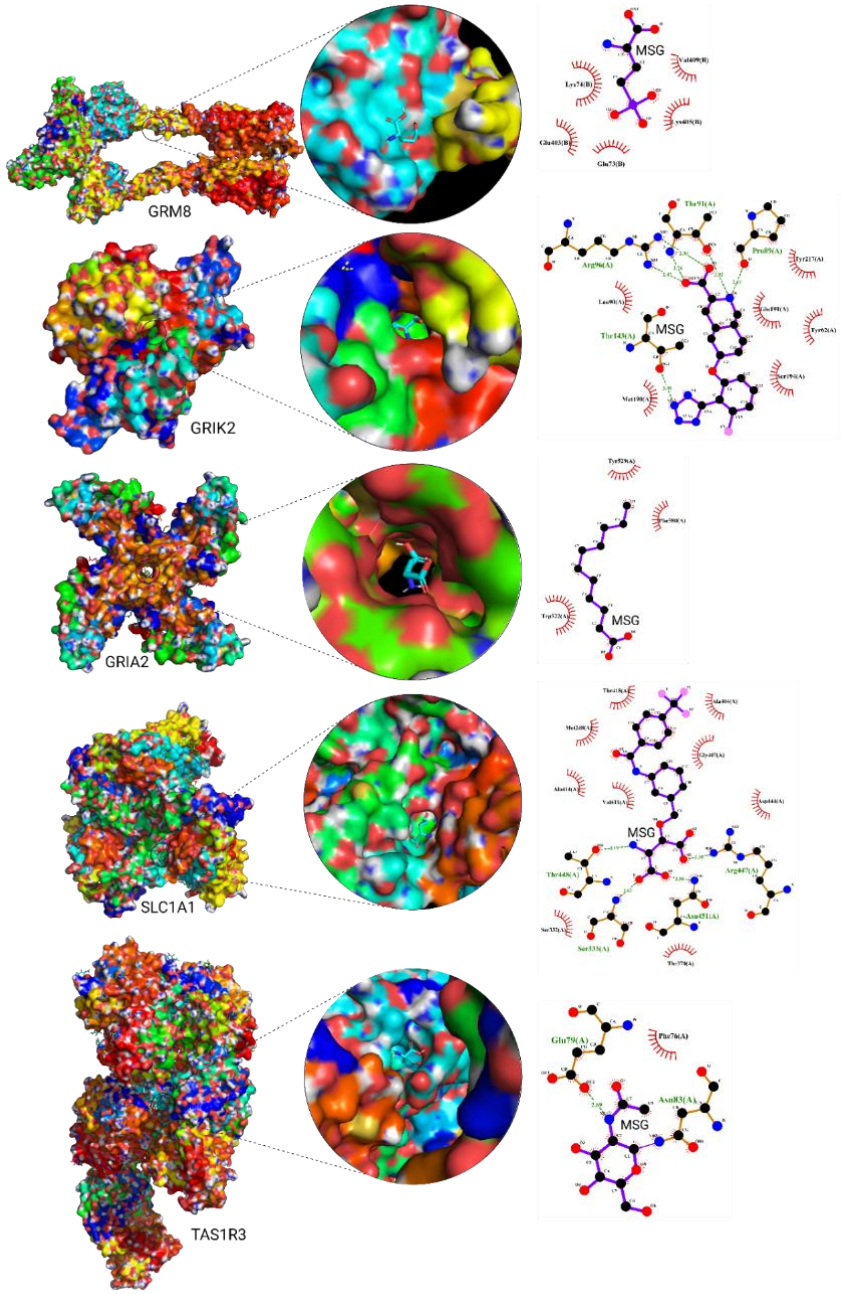

Figure 3 The image illustrates the outcomes of molecular docking analyses for MSG interacting with specific biomolecular targets named GRM8, GRIK2, GRIA2, SLC1A1, and TAS1R3.

The visualization integrates surface models, zoomed interaction sites, and 2D interaction diagrams to present a comprehensive molecular study. The molecular surfaces of the protein targets are visualized with various color schemes to highlight key binding regions. A zoomed-in view is provided of regions of interest where MSG interacts with the protein in order to emphasize the binding pockets. The 2-dimensional schematic diagrams show MSG binding within the target sites, and these representations identify critical amino acid residues that stabilize MSG within the binding pocket. Key hydrogen bonds, hydrophobic interactions, and other intermolecular forces (e.g., van der Waals forces) are mapped and annotated, with specific residues such as Lys, Glu, Thr, Arg, Tyr, and Trp shown to be playing a significant role in the interaction. This analysis is critical for understanding the molecular mechanisms of ligand binding and optimizing ligand modifications for enhanced interaction affinity.

Table 1 The amino acid residue of targets that interacted with MSG and original ligands via hydrogen bonds and hydrophobic contacts.

Gene	Ligand	Binding affinity (kcal/mol)	Hydrophilic interactions	Hydrophobic Contacts
GRM8	$C_5H_8NNaO_4$	−3.3	-	Val409(B), Lys405(B), Lys74(B), Glu403(B), Glu73(B)
GRIK2	$C_5H_8NNaO_4$	−4.8	Arg96(A), Try91(A), Pro89(A), Thr143(A)	Try217(A), Glu191(A), Try62(A), Ser194(A), Leu90(A), Met190(A)
GRIA2	$C_5H_8NNaO_4$	−7.0	-	Thr529(A), Phe580(A), Trp522(A)
SLC1A1	$C_5H_8NNaO_4$	−4.8	Thr448(A), Ser333(A), Asn451(A), Arg447(A)	Thn418(A), Met248(A), Ala414(A), Val411(A), Ala404(A), Gly407(A), Asp444(A), Ser332(A), Thr370(A)
TAS1R3	$C_5H_8NNaO_4$	−4.7	Glu79(A), Asn83(A)	Phe76(A)

Biological activity and ADMET prediction

The ADMET evaluation of the model compound MSG elucidates its pharmacokinetic and toxicity profile, offering insights into its potential for therapeutic development (**Table 2**). High water solubility (log mol/L = −1.37) and robust intestinal absorption (98 % absorbed) underscore its promising bioavailability characteristics. Active blood-brain barrier (BBB) permeability (log BB = 0.79) further suggests the compound's feasibility for central nervous system applications.

Metabolic profiling reveals inactivity across key Cytochrome P450 enzymes as inhibitors and substrates, indicating a reduced likelihood of drug-drug interactions related to these pathways. The compound also exhibits high clearance rates (log mL/min/kg = 0.315), supporting efficient systemic elimination. Toxicity assessments reveal low acute oral toxicity in rat models (LD50 = 4,500 mg/kg) and inactivity in hepatotoxicity and neurotoxicity assays. However, the observed cardiotoxicity warrants targeted investigation to clarify its implications for clinical use. These findings suggest that while MSG demonstrates favorable pharmacokinetic and toxicity parameters for further exploration, attention to cardiotoxic risks remains critical in its developmental trajectory.

Table 2 The ADMET evaluation of the model compound MSG elucidates its pharmacokinetic and toxicity profile, offering insights into its potential for therapeutic development.

Property	Model Name	MSG		Unit
		Predicted Value	Probability	
Absorption	Water solubility	**High**	−1.37	log mol/L
	Intestinal absorption (human)	**High**	0.98	% Absorbed

Property	Model Name	MSG		Unit
		Predicted Value	Probability	
Distribution	BBB permeability	**Active**	0.79	Log BB
Metabolism	CYP1A2 inhibitor	Inactive	99	Yes/No
	CYP2C19 inhibitor	Inactive	99	Yes/No
	CYP2C9 inhibitor	Inactive	95	Yes/No
	CYP2D6 inhibitor	Inactive	88	Yes/No
	CYP3A4 inhibitor	Inactive	99	Yes/No
	CYP2E1 substrate	Inactive	99	Yes/No
Excretion	Total clearance	High	0.315	log mL/min/kg
Toxicity	Oral LD50 (rat)	Low	4,500	mg/kg
	Hepatotoxicity	Inactive	0.79	Yes/No
	Cardiotoxicity	**Active**	0.54	Yes/No
	Neurotoxicity	Inactive	0.78	Yes/No

Investigated the effect of MSG-induced teratogenesis by reducing the ability of cNCCs to synthesize Wnt and BMP signaling proteins

Before entering the next step of the study, we first applied immunofluorescent staining with an anti-HNK-1 antibody specific to cNCCs as shown in **Figures 3** and **4** to determine the precise position of the cNCCs from the cardiac structures that give rise to the pharyngeal arches, aorticopulmonary septum, and cardiac outflow tracts of heart tissue.

We investigated the ability of the cNCCs to synthesize Wnt and BMP signaling proteins; the tissues were stained with different markers using the colocalization of anti-HNK-1, anti-Wnt10B, and anti-BMP-2 protein signaling on ED-3 embryos, as shown in **Figure 4**. Our results indicate that MSG significantly impacts cNCCs by reducing the production of key signaling molecules, Wnt, and BMP proteins. This reduction was statistically significant compared to the control group ($p < 0.05$), as demonstrated by the tissue sections stained with anti-Wnt and anti-BMP markers in **Figure 5**. These results suggest that MSG disrupts the signaling mechanisms of cNCCs by downregulating the synthesis of critical signaling proteins, which could potentially contribute to NCC dysfunction.

Evaluate the impact of MSG exposure on heart morphogenesis

We investigated the effects of MSG on the structural integrity of the embryonic heart. Our findings reveal that MSG exposure results in significant CHDs, including heart wall thinning, impaired septation, and blood congestion. These abnormalities were observed at the early ED-6 stages of embryonic heart development. Quantitative analysis of the left ventricular wall (VW) and interventricular septum (IVS) thickness in ED-6 embryonic hearts demonstrated significant reductions in the MSG group compared to controls and treatment.

The mean VW thickness was 52.86 ± 5.177 and 57.58 ± 8.595 µm in the control group (NSS and FA), 33.21 ± 9.120 µm in the MSG group, and 49.94 ± 3.995 µm in the FA treatment group, with this difference being highly significant ($p < 0.05$). Similarly, the mean IVS thickness in the control group (NSS and FA) was 90.05 ± 2.901 and 79.00 ± 4.710 µm. In contrast, the MSG group exhibited a reduced thickness of 26.72 ± 10.718 µm, and FA treatment group was 53.29 ± 13.11 µm, also achieving statistical significance ($p < 0.05$). These findings are summarized in **Figure 6**.

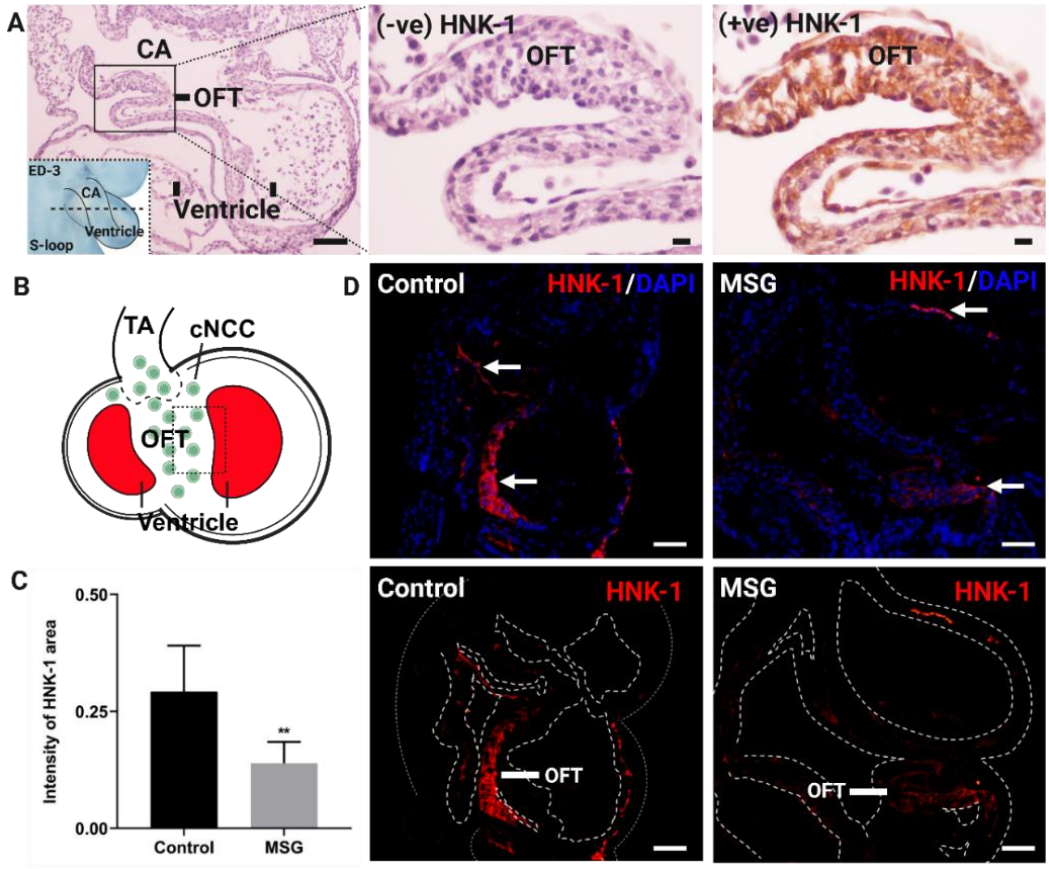

Figure 4 The diagram provides an overview of the investigation into cardiac neural crest cells (cNCC) and their role in heart development, mainly focusing on the cardiac outflow tract (OFT). (A) A dextrodorsal view of ED-3 chick embryos illustrating heart looping, which correlates with the subsequent tissue sections. Immunohistochemical staining identifies the presence of cNCCs on the OFT, providing evidence of their localization indicated by brown staining and highlighting the heart's tissue, including the conus arteriosus (CA), cardiac outflow tract (OFT), and ventricles. This image provides anatomical context for understanding the spatial orientation of the heart during early development. (B) Illustrative diagrams depict the migration of cNCCs through the truncus arteriosus (TA) and into the OFT, showcasing their developmental trajectory. (C) A bar graph compares the intensity of cNCC markers between the control and experimental groups. The results indicate a significant increase in cNCC presence in the experimental groups (** = $p < 0.01$). (D) Sections are labeled with anti-HNK-1 for cNCCs and DAPI for nuclei. Clusters of cNCCs in the OFT are indicated by white arrows. The scale bar is 50 µM, and images are taken at 20× magnification. These comprehensive data provide insights into the distribution, migration, and quantitative changes in cNCCs during cardiac development, emphasizing their crucial role in forming the OFT.

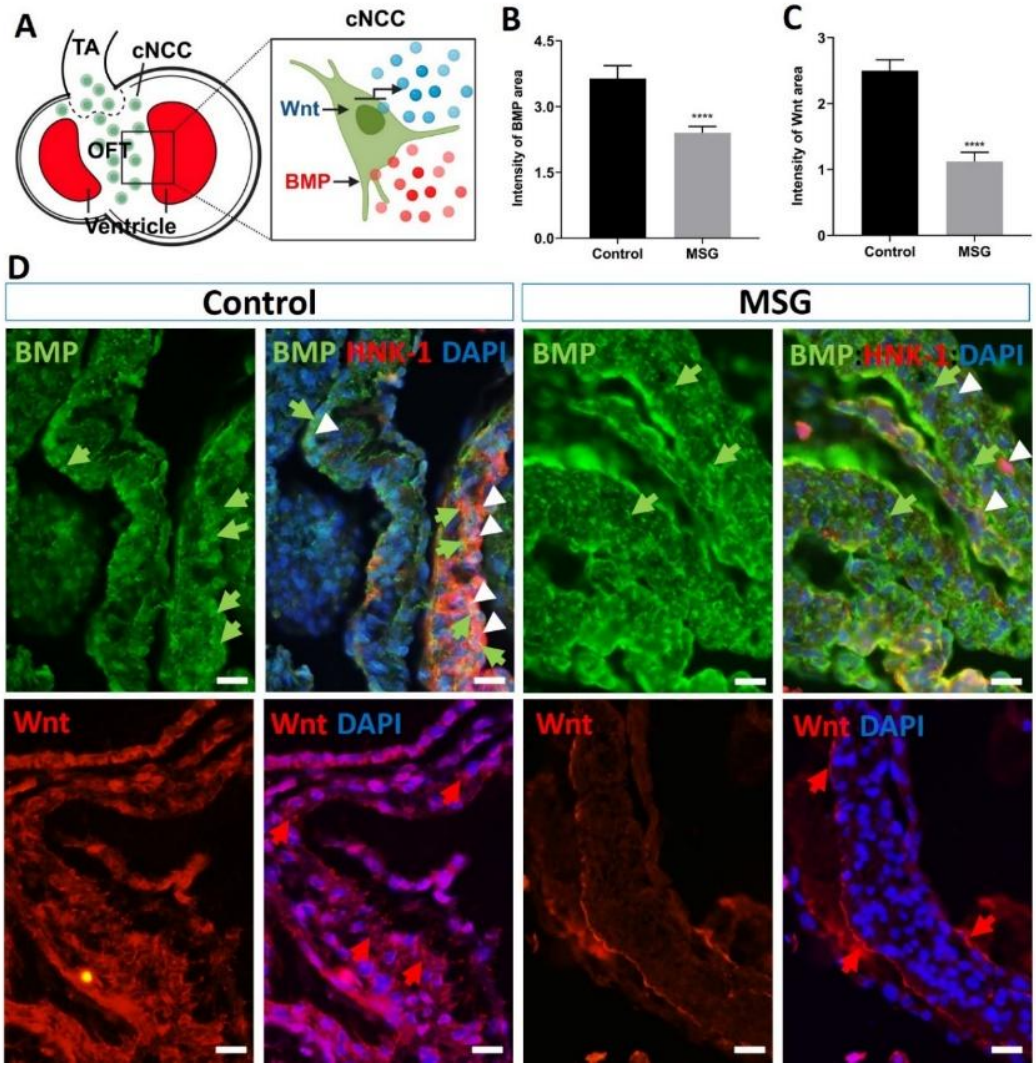

Figure 5 The schematic diagram illustrates the role of protein signaling in heart development. (A) It highlights the signaling pathways of Wnt and BMP proteins produced and released by cNCCs during migration. (C) The bar graph compares the intensities of BMP and Wnt markers between the control and experimental groups, showing a significant reduction in cNCC presence in the experimental group (**** = $p < 0.001$). (D) Immunofluorescent images depict tissue stained with markers for BMP (green arrow), Wnt (red arrow), and the cellular biomarker HNK-1 (white arrow). These images confirm the localization of protein signaling and the presence of NCC. All images were captured at 20× magnification, with a scale bar of 50 µm.

Measured the level of homocysteine in tissues extracted from chick embryos

Our study measured homocysteine (Hcy) levels in chick embryos across various treatment groups and observed a statistically significant elevation in the MSG group compared to the control ($p < 0.005$), and the FA treatment ($p < 0.05$). This increase indicates that MSG, as a teratogen, directly influences tissue and cellular Hcy concentrations, as shown in **Figure 6**. Elevated Hcy levels are a well-documented risk factor for cardiovascular anomalies, supporting the hypothesis that MSG exposure may disrupt normal embryonic development and contribute to the onset of CHDs. Furthermore, the defects were abrogated, and the Hcy reduction was shown when FA was given.

Our results suggest that MSG exposure significantly raises Hcy levels in chick embryos, which may contribute to CHDs. Moreover, the FA plays an important role in controlling Hcy levels in heart tissue.

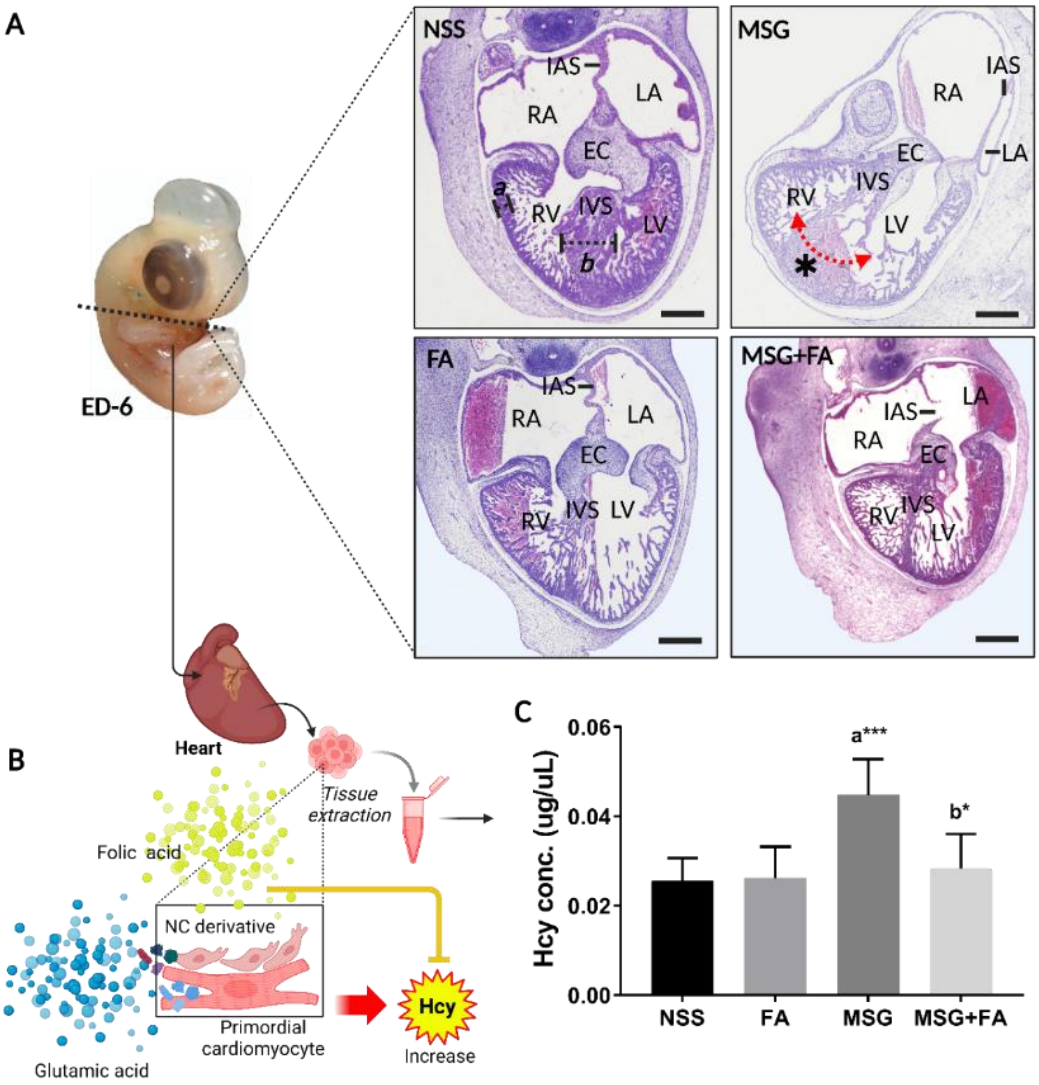

Figure 6 Illustrates histological sections comparing heart morphology between control and MSG exposure embryos at developmental stages of ED-6. (A) shows an overview of an ED-6 embryo, with the dashed line indicating the sectioning plane for the histological analysis. The transverse sections of the heart display in control, MSG, and FA treatment embryos, respectively. The control and FA treatment heart exhibits intact septation with typical structures, including the endocardial cushion (EC), interatrial septum (IAS), interventricular septum (IVS), left atrium (LA), right atrium (RA), left ventricle (LV), and right ventricle (RV). In the MSG group, septal defects are highlighted by red arrows, while an asterisk marks blood congestion in the LA. The heart wall thickness ("a") and septum thickness ("b") are denoted by dashed black lines. The control and FA treatment heart shows well-defined septa and standard wall thickness. In contrast, the MSG heart demonstrates disrupted septation (red arrows), reduced heart wall thickness and septum thickness. Furthermore, the schematic diagram (B) illustrates the homocysteine (Hcy) levels in heart tissues extracted from ED-6 chick embryos. The photograph shows heart tissue dissection for ELISA-based homocysteine determination. The figure depicts the proposed molecular mechanism of MSG-induced cardiovascular defects. MSG exposure increases systemic Hcy levels, as shown in the diagram. Elevated Hcy disrupts endothelial cell integrity, potentially contributing to cardiac malformations. In addition, FA treatment abrogates the adverse effect by reducing Hcy levels. All images were captured at 20× magnification, with a scale bar of 50 µm. The bar graph in (C) presents a comparative analysis of Hcy concentrations (µg/µL) between the control, MSG, and FA treatment groups, revealing a statistically significant increase in Hcy levels in the MSG group (*** = p-value < 0.005, * = p-value < 0.05).

Discussions

This study identified several crucial molecular targets (e.g., GRIM, GRIK, GRIA and others) associated with processes such as cell proliferation, migration, and differentiation. These targets are potentially key players in MSG-induced CHDs. Moreover, pathways involving BMP, nodal/activin, FGF, IGF, and Wnt signaling molecules were implicated in regulating NCCs, which are critical for embryonic development.

This study underscores the significant role of molecular signaling pathways, particularly those mediated by glutamate receptors and GPCR activity, in the etiology of congenital heart defects (CHDs). Identifying 2 overlapping targets from MSG and CHDs from the Venn diagram highlights the mechanistic connections between MSG exposure and CHD pathogenesis. Functional enrichment analysis revealed a strong association of MSG exposure with critical biological processes, including glutamate receptor activity, GPCR activity, and transmembrane signaling receptor activity, which are instrumental in mediating cardiogenesis. These findings suggest that disruptions in these pathways could contribute to abnormal cardiac development and associated neurodevelopmental phenotypes, consistent with findings from previous studies. The molecular docking analysis provided insights into the interaction stability between MSG and specific targets, such as glutamate metabotropic receptor subunit 1 - 5 and glutamate ionotropic receptor kainate type subunit 2. The binding energy values underscore the strong affinity of MSG to these targets, suggesting their involvement in the cardiotoxic effects observed. These observations align with studies highlighting the role of glutamate signaling in developmental disorders and further validate the significance of the identified targets. Moreover, the ADMET analysis revealed promising pharmacokinetic and toxicity profiles for MSG, with notable bioavailability and blood-brain barrier permeability. However, the observed cardiotoxicity necessitates targeted investigations to clarify its implications in clinical and developmental contexts.

Administering a 4 mg concentration of MSG solution per 1 kg of egg weight in 1-day-old chicken embryos exhibited developmental abnormalities through the display of growth retardation, reduced size, craniofacial malformations, heart tube dilation, and delayed limb development [24].

The data suggest MSG disrupts essential molecular pathways and targets, leading to developmental delays and congenital abnormalities. This aligns with the hypothesis that MSG exposure during early development disrupts critical molecular pathways and signaling mechanisms, leading to severe developmental defects. These insights contribute to understanding the mechanisms by which MSG affects embryonic development, especially regarding its teratogenicity.

According to the Centers for Disease Control and Prevention (CDC), CHDs - including atrial and ventricular septal defects, coarctation of the aorta, and tricuspid atresia - have the highest incidence at birth. Abnormalities in NC stem cells are a major contributor to CHDs, and this causal effect has been extensively studied. Previous animal model research found that 34 % of abnormal heart looping cases were associated with MSG-induced teratogenesis [24,26]. Therefore, the present study aimed to investigate the impact of MSG-induced CHDs by exploring its effect on the ability of NC cells to produce Wnt and BMP signaling proteins in a chick embryo model, which closely resembles human heart development.

As corroborated by earlier research, the study identified a decrease in NCC populations, primarily attributed to a significant reduction in NCC cell division. Additionally, the researchers observed a decreased distribution of NCCs across target organs. This decline was associated with reduced production of target proteins such as Wnt and BMP, with a reciprocal effect on NCC behavior. These findings align with the work of Wang *et al*. [27], which highlighted the role of BMP in embryonic growth and disease across body systems. Supporting evidence also comes from Hebert *et al.* [28], who demonstrated the role of a reduction of Wnt in myelomeningocele pathogenesis. Further validation is provided by Zhu *et al.* [29], whose studies explored protein signaling' s regulation of NCC induction and migration processes. The reduced Wnt and BMP levels were also shown to impair the induction process of NCCs.

This study by Itasaki and Hoppler [30] usage highlights the critical role of the Wnt and BMP signaling pathways in biological processes such as stem cell maintenance, cell fate determination, and organogenesis. It emphasizes how integrating these pathways contributes to the complex development and functionality of tissues and organs in the body. Additionally, it notes that the failure to inhibit both Wnt and BMP signaling pathways in animal models disrupts proper head formation, resulting in malformed head structures [31]. This underscores the necessity of precise regulation in these pathways for normal development and organogenesis.

We have discovered MSG's impact on NCCs and the related signaling pathways. Our research reveals a previously unreported effect of MSG by reducing the activity of neural crest cells (NCCs), leading to decreased production of critical signaling proteins, including Wnt and BMP. This decline in signaling disrupts the inhibitory control exerted by NCCs, impairing their proliferation and altering specific cellular functions. These findings provide new evidence linking MSG exposure to CHDs through the modulation of signaling protein production.

MSG exposure significantly disrupts embryonic heart development, as evidenced by septal defects, myocardial thinning, and blood congestion observed in treated embryos at ED-6. These abnormalities likely result from the disruption of critical signaling pathways, such as Wnt/β-catenin and TGF-β, which are essential for cardiac septation and remodeling [32,33], as well as oxidative stress-induced damage to myocardial and endothelial cells [34,35]. The progressive nature of these defects suggests the cumulative effects of MSG on cardiac development over time [36]. Furthermore, blood congestion in the left atrium indicates impaired hemodynamics, likely caused by defective septation and chamber remodeling [37]. These findings highlight the potential teratogenic effects of MSG, with implications for understanding environmental risk factors contributing to congenital heart defects in humans [38,39].

Imbalances influence congenital disabilities in homocysteine (Hcy), folate, and vitamin B12 levels, which result in embryonic abnormalities [40,41]. Our study quantified Hcy levels in tissues extracted from the heart tissue of 6-day-old chick embryos. The results indicated significantly elevated Hcy concentrations in the MSG group and reduced Hcy concentrations in the FA-treatment group. Teratogens such as MSG directly affect tissue and cellular Hcy levels, ultimately contributing to CHDs. These findings align with Iacobazzi *et al.* [43], who reported that elevated Hcy in the bloodstream led to embryonic abnormalities in animal testing [42]. Furthermore, the relationship between Hcy and cellular activity is critical during organogenesis. Increased Hcy levels inversely correlate with the cellular regulation of gene expression and programmed cell death, resulting in a cessation of cell activity and the development of congenital BDs [44].

Folic acid acts as an essential cofactor in the remethylation of homocysteine to methionine, enhancing the activity of enzymes like methylene tetrahydrofolate reductase (MTHFR) and cystathionine β-synthase. Thus, it mitigates the adverse effects of elevated Hcy [45]. These results are particularly relevant for populations with dietary folate deficiencies or those consuming high levels of MSG, which could exacerbate health issues related to Hcy. These findings underscore the importance of sufficient folate intake as a modifiable factor in managing Hcy levels and reducing associated CHD risks.

Conclusions

In conclusion, this study provides novel insights into the mechanistic interplay between MSG exposure, NCC disruption, the treatment role of FA, and CHD pathogenesis through shared molecular pathways. This study contributes significantly to understanding MSG-induced teratogenicity, emphasizing its role in connecting molecular targets, signaling disruptions, and biochemical imbalances to developmental defects. By focusing on NCC dysfunction and the critical role of Wnt and BMP pathways, the research bridges significant gaps in knowledge about MSG's impact on embryonic development and its implications for CHDs. The findings reinforce the need to further explore MSG's effects on human development and the broader implications for dietary and environmental exposures during pregnancy. Future research should aim to validate these findings in experimental models and explore the translational potential of targeting identified pathways for therapeutic interventions.

Acknowledgements

We would like to thank the research staff of the faculty of medicine, Princess of Narathiwas University, Thailand for supporting each technique performed in this research. The facilities are supported by the faculty of medicine, Princess of Narathiwas University. This research was funded by medical research fund 2022 from Faculty of Medicine Princess of Naradhiwas University for providing financial support.

References

[1] Y Liu, S Chen, L Zühlke, GC Black, MK Choy, N Li and BD Keavney. Global birth prevalence of congenital heart defects 1970 - 2017: Updated systematic review and meta-analysis of 260 studies. *International Journal of Epidemiology* 2019; **48(2)**, 455-463.

[2] R Kučienė and V Dulskienė. Selected environmental risk factors and congenital heart defects. *Medicina* 2008; **44(11)**, 827.

[3] S Baldacci, F Gorini, M Santoro, A Pierini, F Minichilli and F Bianchi. Environmental and individual exposure and the risk of congenital anomalies: A review of recent epidemiological evidence. *Epidemiologia e Prevenzione* 2018; **42(3-4)**, 1-34.

[4] LX Liu and Z Arany. Maternal cardiac metabolism in pregnancy. *Cardiovascular Research* 2014; **101(4)**, 545-553.

[5] F Lamberto, I Peral-Sanchez, S Muenthaisong, M Zana, S Willaime-Morawek and A Dinnyés. Environmental alterations during embryonic development: Studying the impact of stressors on pluripotent stem cell-derived cardiomyocytes. *Genes* 2021; **12(10)**, 1564.

[6] TP Fleming, C Sun, O Denisenko, L Caetano, A Aljahdali, JM Gould and P Khurana. Environmental exposures around conception: Developmental pathways leading to lifetime disease risk. *International Journal of Environmental Research and Public Health* 2021; **18(17)**, 9380.

[7] SP Chakraborty. Patho-physiological and toxicological aspects of monosodium glutamate. *Toxicology Mechanisms and Methods* 2019; **29(6)**, 389-396.

[8] S Erhardt, M Zheng, X Zhao, TP Le, TO Findley and J Wang. The cardiac neural crest cells in heart development and congenital heart defects. *Journal of Cardiovascular Development and Disease* 2021; **8(8)**, 89.

[9] HSW Haroun. Teratogenicity and teratogenic factors. *MOJ Anatomy and Physiology* 2017; **3(1)**, 1-5.

[10] AS Mahaliyana, MFA Fasmina, AMTB Alahakoon and GMGMM Wickrama. Toxicity effects of monosodium glutamate (MSG) on embryonic development of zebrafish (Danio rerio); A promising model to study excitotoxins. *International Journal of Scientific and Research Publications* 2016; **6(3)**, 229-234.

[11] NAA Elnaga, M Sarhan and H Mansour. Teratogenicity of monosodium glutamate on pregnant rats and their fetuses. *The Egyptian Journal of Hospital Medicine* 2019; **74(8)**, 1737-1747.

[12] S Cerrizuela, GA Vega-Lopez and MJ Aybar. The role of teratogens in neural crest development. *Birth Defects Research* 2020; **112(8)**, 584-632.

[13] E Takimoto and DA Kass. Role of oxidative stress in cardiac hypertrophy and remodeling. *Hypertension* 2007; **49(2)**, 241-248.

[14] S Pintarasri, M Santiparadon, A Kamnate, C Naktubtim, T Koomsang and W Payuhakrit. A novel's evidence of Msg-induced craniofacial defects in chick embryo models. *Trends in Science* 2024; **21(12)**, 8718.

[15] TL Creazzo, RE Godt, L Leatherbury, SJ Conway and ML Kirby. Role of cardiac neural crest cells in cardiovascular development. *Annual Review of Physiology*1998; **60**, 267-286.

[16] AL Hopkins. The role of network pharmacology in understanding multifactorial diseases. *Nature Reviews Drug Discovery* 2022; **21(1)**, 39-56.

[17] X Chen, CC Yan, X Zhang, X Zhang, F Dai, J Yin and Y Zhang. Drug-target interaction prediction: Databases, web servers and computational models. *Briefings in Bioinformatics* 2016; **17(4)**, 696-712.

[18] J Lin and H Nagase. The road not taken with pyrrole-imidazole polyamides: Off-target effects and genomic binding. *Biomolecules* 2020; **10(4)**, 544.

[19] A Negri, V Naponelli, F Rizzi and S Bettuzzi. Molecular targets of epigallocatechin - Gallate (EGCG): A special focus on signal transduction and cancer. *Nutrients* 2018; **10(12)**, 1936.

[20] W Tang, ML Martik, Y Li and ME Bronner. Cardiac neural crest contributes to cardiomyocytes in amniotes and heart regeneration in zebrafish. *Elife* 2019; **8**, e47929.

[21] O Schussler, L Gharibeh, P Mootoosamy, N Murith, V Tien, AL Rougemont, T Sologashvili, E Suuronen, Y Lecarpentier and M Ruel. Cardiac neural crest cells: Their rhombomeric specification, migration, and association with heart and great vessel anomalies. *Cellular and Molecular Neurobiology* 2021; **41(2)**, 403-429.

[22] ME Bronner and NM LeDouarin. Development and evolution of the neural crest: An overview. *Developmental Biology* 2012; **366(1)**, 2-9.

[23] R Pal and A Khanna. Role of smad-and wnt-dependent pathways in embryonic cardiac development. *Stem cells and Development* 2006; **15(1)**, 29-39.

[24] A Mohan, R Kumar, V Kumar and M Yadav. Homocysteine, vitamin B12 and folate level: Possible risk factors in the progression of chronic heart and kidney disorders. *Current Cardiology Reviews* 2023; **19(4)**, 66-83.

[25] S Pintarasri, V Plakornkul, Y Viravud, W Payuhakrit and T Rungruang. Folic acid attenuates MSG-induced teratogenicity during a 2-month pregnancy by preventing neural crest cell destruction and malformation in chick embryo models. *Trends in Sciences* 2023; **20(7)**, 6656.

[26] SM Hazzaa, ES El-Roghy, MA Abd Eldaim and GE Elgarawany. Monosodium glutamate induces cardiac toxicity via oxidative stress, fibrosis, and P53 proapoptotic protein expression in rats. *Environmental Science and Pollution Research* 2020; **27(17)**, 20014-20024.

[27] RN Wang, J Green, Z Wang, Y Deng, M Qiao, M Peabody, Q Zhang, J Ye, Z Yan, Z Yan, S Denduluri, O Idowu, M Li, C Shen, A Hu, RC Haydon, R Kang, J Mok, MJ Lee, HL Luu and LL Shi. Bone morphogenetic protein (BMP) signaling in development and human diseases. *Genes & Diseases* 2014; **1(1)**, 87-105.

[28] L Hebert, P Hillman, C Baker, M Brown, A Ashley-Koch, JE Hixson, AC Morrison, H Northrup and KS Au. Burden of rare deleterious variants in WNT signaling genes among 511 myelomeningocele patients. *PLoS One* 2020; **15(9)**, e0239083.

[29] XJ Zhu, YD Liu, ZM Dai, X Zhang, XQ Yang, Y Li, M Qiu, J Fu, W Hsu, YP Chen and Z Zhang. BMP-FGF signaling axis mediates Wnt-induced epidermal stratification in developing mammalian skin. *PLoS Genetics* 2014; **10(10)**, e1004687.

[30] N Itasaki and S Hoppler. Crosstalk between Wnt and bone morphogenic protein signaling: A turbulent relationship. *Developmental Dynamics: An Official Publication of the American Association of Anatomists* 2010; **239(1)**, 16-33.

[31] G Chen, C Deng and YP Li. TGF-β and BMP signaling in osteoblast differentiation and bone formation. *International Journal of Biological Sciences* 2012; **8(2)**, 272-288.

[32] IA Mohamed, N El-Badri and A Zaher. Wnt signaling: The double-edged sword diminishing the potential of stem cell therapy in congenital heart disease. *Life Sciences* 2019; **239**, 116937.

[33] Y Li, J Du, S Deng, B Liu, X Jing, Y Yan, Y Liu, J Wang, X Zhou and Q She. The molecular mechanisms of cardiac development and related diseases. *Signal Transduction and Targeted Therapy* 2024; **9(1)**, 368.

[34] S Silvestro, V Calcaterra, G Pelizzo, P Bramanti and E Mazzon. Prenatal hypoxia and placental oxidative stress: insights from animal models to clinical evidences. *Antioxidants* 2020; **9(5)**, 414.

[35] N Mollo, R Scognamiglio, A Conti, S Paladino, L Nitsch and A Izzo. Genetics and molecular basis of congenital heart defects in Down syndrome: Role of extracellular matrix regulation. *International Journal of Molecular Sciences* 2023; **24(3)**, 2918.

[36] S Sambu, U Hemaram, R Murugan and AA Alsofi. Toxicological and teratogenic effect of various food additives: An updated review. *BioMed Research International* 2022; **2022**, 6829409.

[37] JI Hoffman and S Kaplan. The incidence of congenital heart disease. *Journal of the American College of Cardiology* 2002; **39(12)**, 1890-1900.

[38] A Zanfirescu, A Ungurianu, AM Tsatsakis, GM Nițulescu, D Kouretas, A Veskoukis, D Tsoukalas, AB Engin, M Aschner and D Margină. A review of the alleged health hazards of monosodium glutamate. *Comprehensive Reviews in Food Science and Food Safety* 2019; **18(4)**, 1111-1134.

[39] GJ Udom, BR Abdulyekeen, MO Osakwe, AN Ezejiofor, CN Orish, FC Orish, C Frazzoli and OE Orisakwe. Reconsideration of the health effects of monosodium glutamate: From bench to bedside evidence. *Journal of Environmental Science and Health, Part C* 2024; **43**, 1-31.

[40] A Mahajan, D Sapehia, S Thakur, PS Mohanraj, R Bagga and J Kaur. Effect of imbalance in folate and vitamin B12 in maternal/parental diet on global methylation and regulatory miRNAs. *Scientific Reports* 2019; **9(1)**, 17602.

[41] B Li, Y Xu, D Pang, Q Zhao, L Zhang, M Li, W Li, G Duan and C Zhu. Interrelation between homocysteine metabolism and the development of autism spectrum disorder in children. *Frontiers in Molecular Neuroscience* 2022; **15**, 947513.

[42] PR Brauer and BJ Tierney. Consequences of elevated homocysteine during embryonic development and possible modes of action. *Current Pharmaceutical Design* 2004; **10(22)**, 2719-2732.

[43] V Iacobazzi, V Infantino, A Castegna and G Andria. Hyperhomocysteinemia: Related genetic diseases and congenital defects, abnormal DNA methylation and newborn screening issues. *Molecular Genetics and Metabolism* 2014; **113(1-2)**, 27-33.

[44] RM Shawky, AR Ramy, SMN El-Din, SM Abd Elmonem and MA Abd Elmonem. Abnormal maternal biomarkers of homocysteine and methionine metabolism and the risk of congenital heart defects. *Egyptian Journal of Medical Human Genetics* 2018; **19(1)**, 7-12.

[45] L Koklesova, A Mazurakova, M Samec, K Biringer, SM Samuel, D Büsselberg, P Kubatka and O Golubnitschaja. Homocysteine metabolism as the target for predictive medical approach, disease prevention, prognosis, and treatments tailored to the person. *EPMA Journal* 2021; **12**, 477-505.